Journal of Environmental Chemical Engineering 10 (2022) 107423

Contents lists available at ScienceDirect

Journal of Environmental Chemical Engineering

journal homepage: www.elsevier.com/locate/jece

Thin film nanocomposite membrane incorporated with clay-ionic liquid framework for enhancing rejection of epigallocatechin gallate in aqueous media

Alimpia Borah [a,b], Monti Gogoi [a,b], Rajiv Goswami [a,b], Hrishikesh Sarmah [a], Krishna Kamal Hazarika [a], Swapnali Hazarika [a,b,*]

[a] Chemical Engineering Group, Engineering Sciences & Technology Division CSIR-North East Institute of Science and Technology, Jorhat 785006, Assam, India
[b] Academy of Scientific and Innovative Research (AcSIR), Ghaziabad 201002, India

ARTICLE INFO

Editor: Despo Kassinos

Keywords:
Polyamide
Interfacial polymerization
Epigallocatechin gallate
Rejection
Flux

ABSTRACT

Tea catechins are the major ingredients in tea polyphenols. The design of nanomaterials from natural resources for versatile applications is a global topic of research. Here, we have reported a new and versatile Thin Film Nanocomposite (TFN) membrane that was developed from ionic liquid functionalized bentonite clay. Clay-[1-hexyl-3-methylimidazolium chloride] framework was introduced as a nano additive to prepare high performance TFN membranes of thermal stability 630 °C. The polyamide layer was designed over the membrane surface for selective separation of epigallocatechin gallate (EGCG). In this work, diffusive mass transfer across porous hydrophilic surfaces is significant in an emerging trade-off between membrane flux and permeability for selective separation of EGCG. The membrane showed 94% rejection at pressure 5 bar, flow rate of 23 mL.min^{-1} and feed concentration of 1.5 mmol.L^{-1}. The membrane showed its efficiency for its reusability. This study confirms the desirable applicability of novel functionalized bentonite (FBn) based TFN membranes for selective separation of biomolecule in aqueous media.

1. Introduction

It is a well-known fact that green tea is the best possible source of tea polyphenols, where % of tea polyphenols are found to be 45–90% [1]. Tea polyphenols have a lot of demand for different physiological and pharmacological effects [1,2]. Green tea polyphenols contain different catechin compositions like epicatechin (EC), epigallocatechin (EGC), gallocatechin gallate (GCG), epicatechin gallate (ECG) and epigallocatechin gallate (EGCG). Among these, the most persuasive antioxidant is EGCG, and its contents are comparatively more than other catechins in green tea [2]. The special beneficial effect exhibited by tea polyphenols includes anticancer, anti inflammatory and antioxidant effects. In tea, the percentage of catechin components for EGCG has been estimated as 30–50% [3,4].

It is a challenge to separate the pure compounds of tea catechins with improved activity. Although conventional methods like solvent extraction under microwave and ultrasound, high-performance liquid chromatography, and adsorption can separate the tea polyphenol in natural usage, these are tedious and energy excessive processes [5–7]. A. Kumar et al. reported the separation of epigallocatechin gallate through a two phase infused membrane process. They have used ultrafiltration membrane to extract a maximum of 80% of EGCG from tea powder [8]. M.S. Manna et al. evaluated the separation of medicinal catechins from green tea extract using a hollow fiber supported liquid membrane. They have evaluated the mass transfer parameter to study the recovery of all tea catechins [9]. To the best of our knowledge, no such work has been reported for the membrane based separation of epigallocatechin gallate till date. This process may lead to the cost effective route to separate the individual catechin at a better quantitative rate. The use of promising membrane technology has gained remarkable attention due to the trade-off between water flux and satisfying rejection of reactive biomolecule and scalability's scope [10]. Therefore, efforts have been made to address this issue considering the modern separation technique through TFN based processes. Further, this process has gained high demand for developing thin film nanocomposite membranes in recent years. The TFN membranes are highly energy efficient and have low

* Corresponding author at: Chemical Engineering Group, Engineering Sciences & Technology Division CSIR-North East Institute of Science and Technology, Jorhat 785006, Assam, India.
E-mail address: shrrljt@yahoo.com (S. Hazarika).

https://doi.org/10.1016/j.jece.2022.107423
Received 29 December 2021; Received in revised form 11 February 2022; Accepted 15 February 2022
Available online 6 March 2022

pressure driven separation barriers on the ambitious flow of separation science [11]. It is reported that the separation behavior was sometimes limited due to chemical interaction within the polymeric materials used to prepare support substrate [12]. Efforts have been made to design and fabricate the TFN membrane using nanofillers into the reactive platform. Researchers have also tried to address the interfacial polymerization process for developing thin film nanocomposite membranes of excellent performance [13]. Therefore, we have emphasized the development of the TFN membrane from novel materials for separating tea catechins in aqueous media.

On the contrary, this is a step growth condensation polymerization and propagates through an interface of two immiscible liquid media, which can endow the polymeric substrate with a unique anisotropic shape and alternative surface chemistry [14]. This process is an effective and robust approach to trigger the polymeric material compared to the bulk polymerization [15,16]. Monomers including amide, ester, aniline, alkene can be widely used for Interfacial Polymerization (IP) process and can establish some reactive network of amide, ester layer, etc. [15]. During interfacial polymerization process, thin film nanocomposite (TFN) membranes are formed through the addition of nanofiller into the selective layer. The nanofillers can be embedded over polyamide layer through its addition into one of the monomer solutions. Depending upon the solubility or dispersion ability of nanofiller, it will be added into corresponding aqueous or organic layer. Herein, the incorporation of functionalized clay may enhance the permeability and solute rejection that could be better compared to the typical TFC membrane. Normally, porous or nonporous nanoparticles can be used as nanofiller into the IP process. These nanofiller can possess significant changes in the physicochemical properties of polymeric layer (polyamide, polyester) and also transport properties of TFN membranes. Whereas, the nonporous nanofiller such as metal oxide nanoparticles (TiO_2, SiO_2) can compromise with permeability due to an increase of water resistance properties. The addition of nanofiller into each of the monomer media can overall effect on the stability and chemical reactivity of formed polymer layer. Introduction of nanofiller into the selective coating, which is formed due to the polymerization, can induce the alternative pathway to increase the mass transfer rate via intrinsic nanosized pore or interface void between amide layer and nanofiller [16].

Instead of using the nanofillers as a solvent in any monomeric solutions, they can also be considered as additive to facilitate their phase transfer catalytic behavior over the outer layer of the polyamide formation process [17–19]. Following the IP process, the uneven polyamide layer formed over the polymeric substrate could be the reason for the thin film membrane performance deterioration. Therefore, researchers have put in numerous efforts to optimize the surface properties, including the addition of hydrophilic additives, bending of hydrophobic components, adjusting the pore size of the substrate, and wettability of surface properties [20,21].

X. J. Kong et al. reported the preparation of Boronate Affinity (BA) membrane via immobilization of bromine groups on nylon 66 membrane through grafting of poly(4-vinylphenylboronic acid) chains [22]. T. Zhang et al. reported on the preparation of ionic liquid and β-cyclodextrin based membrane for the separation of total tea polyphenol from crude extract of green tea. IL@β-CD-Gel membrane showed the adsorption capacity for TPs was 303.45 mg/g with removal percentages of 94.38% [23]. These reported works mainly based on the thermodynamics analysis of total polyphenol content extracted from crude tea extract. In our case, we have prepared TFN membranes through IP process for selective separation of individual polyphenol.

Our work intends to develop an Ionic Liquid (IL)-clay-based TFN membrane on polysulfone support, which is highly propitious and valuable for separating polyphenols. The IL has a greater tendency to exfoliate the stacked clay sheets due to the intercalation of the long alkyl chain. It can possess intermolecular attraction with a hydroxyl group of stacked clay sheets [24,25]. Therefore, our ongoing research has shown the preparation of thin film nanocomposite membranes through interfacial polymerization process, initiated via aqueous monomeric meta phenylene diamine (MPD) solution with an organic solution of adipoyl chloride. We used organoclay composite into the aqueous monomeric solution varying the wt% of organoclay for the adequate mass transfer performance into the interphase of two monomers. It suggests that introducing 0.4 wt% of IL-clay composite into the aqueous monomeric solution can help to form an organic core microcapsule and entrap the molecule on a polymeric substrate which can be recovered by backwashing [24]. The developed membranes were undertaken to address their separation performance on tea catechin EGCG. During membrane treatment, we observed that M_{FBn2} exhibited better performance with a high flux recovery ratio because the introduction of IL added clay into the aqueous monomeric solution has shown better monomer diffusion inside the organic phase. The highly acceptable behavior of IL is due to its lower surface tension [25], high solubility and dissolution tendency in MPD monomer and surfactant properties. The top polymeric layer of amide linkage could give excellent water permeability and lower antifouling tendency [26]. Here, we have also illustrated the mechanism that evolved during the permeation experiment and quantified the rejection % profile of EGCG. We have included the salt rejection study in our work as the salt rejection is the preliminary study of nanofiltration membrane. It can explore the evidences of various physicochemical properties of membrane. The surface charge property of membrane is very much essential to describe the salt rejection performance of membrane [27,28].

2. Materials and methods

2.1. Materials

Hydrophilic bentonite nanoclay (≤25 μm), epigallocatechin gallate ($C_{22}H_{18}O_{11}$, >98%, HPLC) and polysulfone (PSf) was purchased from M/s Sigma Aldrich. Ionic liquid 1-hexyl-3-methylimidazolium chloride [$C_{10}H_{19}ClN_2$, ≥ 97.0% (HPLC)] was purchased from Merck. Milli-Q deionized water was used throughout the experiments. The polyethylene glycol and organic solvent N-methylpyrollidone (NMP) were obtained from M/s TCI Chemicals (India) Pvt. Ltd. Metaphenylene diamine (MPD, $C_6H_4(NH_2)_2$) and adipoyl chloride ($C_6H_8Cl_2O_2$) used as the monomer for polymerization reaction were procured from M/s Sisco Research Laboratory Pvt. Ltd (SRL), India. n-Hexane used as solvent was obtained from M/s RANKEM range of laboratory chemicals, Gujarat, India.

2.2. Method

2.2.1. Preparation of the organoclay (modified bentonite clay)

For functionalization of bentonite clay, 4 g of activated raw clay particle was dispersed in a solution of ionic liquid 1-hexyl-3-methylimidazolium chloride 12% v/v in methanol. It was continuously stirred at constant stirring for 2 h. Furthermore, the clay solution was ultrasonicated to exfoliate their stacked sheets. The solution mixture was allowed to undergo centrifugation for 10 min so that there was a significant separation between the solid and liquid phases. The suspended clay was filtered using filter paper and washed thoroughly with methanol several times. The filtered solids were dried at around 110 °C temperature for 12 h.

2.2.2. Fabrication of thin film nanocomposite membrane

23% of polysulfone was dissolved in NMP under vigorous stirring at a temperature of 40 °C. The homogenization of polymeric solution was done by continuous stirring. After that, the solution mixture was separated into two parts. One part of the solution was cast on a clean glass plate throughout the degassing atmosphere, and a fraction of bentonite was added to another part of the polymeric solution. The clay based polymeric solution was cast on a glass plate and dipped in a clean water bath of deionized water. During this time, a higher degree of phase

separation occurred, and the solid membrane was obtained. The membranes were dipped in a water bath for 24 h and then oven dried for further use. Bare polysulfone membrane was denoted as M_{PSf} and membrane containing raw bentonite was denoted as M_{Bn}.

The TFN membranes were prepared by the interfacial polymerization method. The process was initiated by preparing two different monomer solutions at a ratio of 2:1. In an aqueous solution of MPD (0.6% w/v), 0.2, 0.4 and 0.6 wt% of clay-[1-hexyl-3-methylimidazolium chloride] was added separately and dispersed. The three solutions were individually poured over the top surface of the PSf membrane and left for 5 min to ensure diffusion through membrane support. The excess solution was removed from the membrane and then poured 0.3% (w/v) solution of adipoyl chloride in hexane on the treated membrane and dried. The resulting membranes were cured at 70 °C for 10 min to promote more cross linking of Polyamide (PA) over the membrane surface. The fabricated TFN membranes containing 0.2 wt%, 0.4 wt% and 0.6 wt% of IL-clay are denoted as M_{FBn1}, M_{FBn2} and M_{FBn3} respectively. The two surface active monomers MPD and adipoyl chloride was taken for interfacial polymerization process, as shown in Figs. 1 and 2.

2.2.3. Studies on intrinsic properties of TFN membrane

Fourier Transform Infrared Spectroscopy (FTIR) was used to determine the functional groups present in pristine clay, organoclay and prepared TFN membranes using Perkin Elmer, 2000 Infrared spectrophotometer. The spectrum was recorded in the range of 800–4000 cm^{-1}. To examine the elemental composition and binding energy of organoclay and prepared thin film surfaces, a quantitative spectroscopic technique, X-ray Photoelectron Spectroscopy (XPS), was used. The spectroscopic analysis was conducted using Thermo Fisher Scientific: ESCALAB Xi+ , equipped with a monochromated Al Kα radiation. The surface morphology of prepared organoclay and cross sectional view of TFN membranes was studied using field emission scanning electron microscopy (FESEM, LEO 1427 VP, UK) at an accelerating voltage of 3 kV. The samples were scanned after covering with a thin layer of conducting gold using sputtering apparatus. The microscopic image of the prepared organoclay was determined using high resolution transmission electron microscopy (HRTEM, JEOL, Japan, JEM 2100). Brunauer Emmett Teller (BET) nitrogen adsorption-desorption technique was used to determine the porosity of the membrane surface and the surface area of the mesoporous membrane surface. Based on the principle of physical gas adsorption, the surface area of thin film nanocomposite membranes was determined using Quantachrome® AsiQwin™- Automated Gas Sorption instrument. Thermogravimetric analysis (TGA) was done to determine the polymer degradation temperature and thermal stability of TFN membranes under a nitrogen atmosphere up to 700 °C at a heating rate of 20 °C/min. Sur PASS™ Electrokinetic Analyzer (Anton Paar, Austria) was used to determine the electrokinetic potential of polymeric samples. The charge effect over the membrane surface was analyzed by determining streaming potential and current measurement using Helmholtz-Smoluchowski Equations. The electrokinetic potential created on the thin film membrane surface was measured in terms of Zeta potential (ζ). The water contact angle at the liquid and solid membrane surface interface was determined by the sessile drop method using a contact angle meter (DM-501, Kyonea Interface Science) at 25 °C. The pristine and modified thin films were treated with deionized water as probe liquid. The angle was randomly measured at different positions of the membrane surface and their average was reported as contact angle. The mechanical properties of prepared membranes were determined by the Universal Tensile Testing Machine (AEC 1112-5 KN ACD), which can measure the force of compressive or transverse stresses.

2.2.4. Separation of epigallocatechin gallate (EGCG)

Membrane permeation experiments for separation of epigallocatechin gallate were carried out through a dead-end membrane set up made up of SS 316 having two compartments of cylindrical shape. A circular section of the membrane was fitted between both the compartments. The effective surface area of the membrane was 18.32 cm^2. The flow rate was controlled by a peristaltic pump appropriately calibrated and maintained the pressure by a pressure controller. The membrane permeation experiments were conducted under a nitrogen gas atmosphere. The sample was collected from the permeate side at a definite time interval and measured their absorbance value using UV visible spectrophotometer (Thermo scientific, evolution 201). After each experiment, the membrane was back washed using deionized water for its reusability. Fig. 3 depicts the schematic representation of the permeation set-up. The pure water permeability of each membrane was determined using the same experimental set-up.

The prepared nanocomposite membranes were used to evaluate the rejection rate of tea catechin under the optimum condition of physicodynamic parameters, including temperature, pressure and flow rate. The pure water permeability and catechin rejection performance of each membrane was studied separately and each permeation experiment was conducted for 8 h in a continuous mode of feed flow. Samples were collected every interval of 1 h and concentration of the permeate was estimated using UV visible spectroscopy. Based on the data obtained from the analysis, the membrane permeation flux and rejection (%) were calculated using the standard equation mentioned in our previous publication [29].

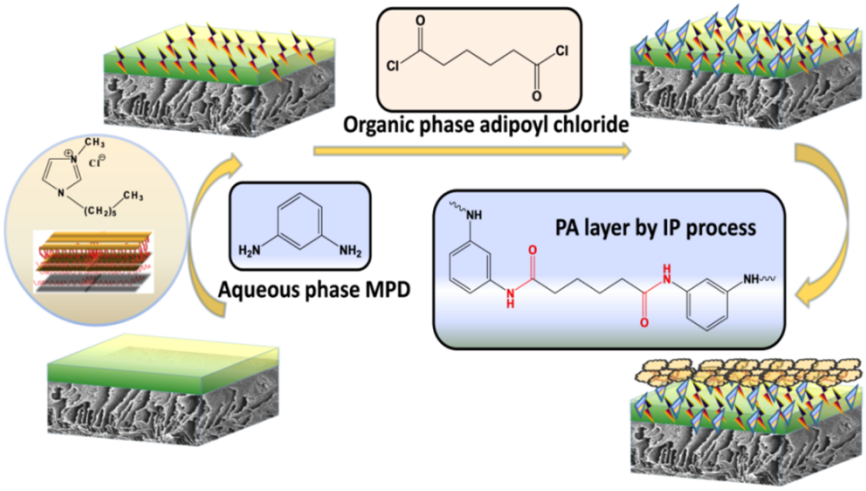

Fig. 1. Schematic diagram of Interfacial polymerization process.

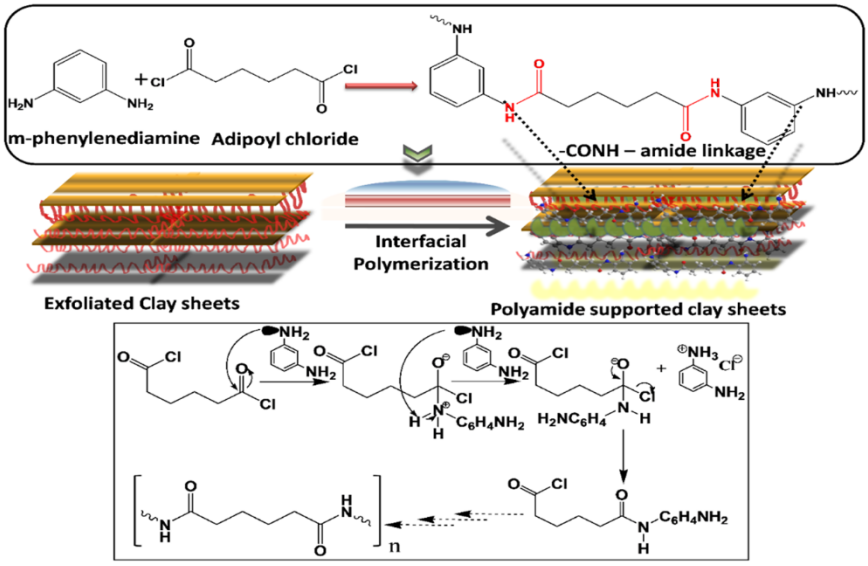

Fig. 2. Reaction scheme for the formation of amide linkage between two monomers.

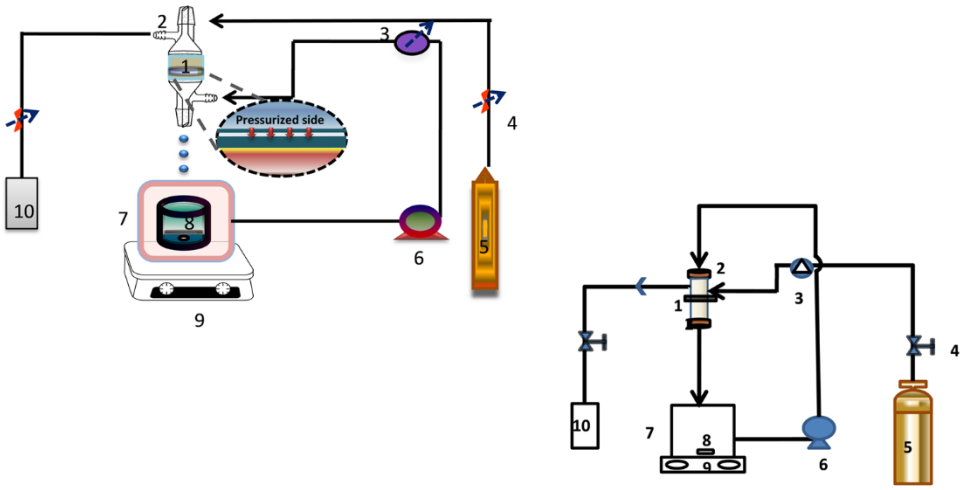

Fig. 3. Schematic representation of the permeation set-up (1) Membrane, (2) Membrane cell, (3) Pressure gauze, (4) Valve, (5) Nitrogen cylinder, (6) Peristaltic pump, (7) Feed tank, (8) Magnetic needle, (9) Magnetic stirrer and (10) Gas outlet.

2.2.5. Long term test of membranes

The long term test of the prepared membranes was carried out to determine stability and efficiency of membrane for separation of EGCG. The long term performance of the membrane was analysed over a period of 6 months. For this purpose, the membrane was dipped in aqueous solution of EGCG for a definite period of time and then membrane flux was determined using membrane permeation set up as shown in Fig. 3. The membranes were regenerated prior to the use.

2.2.6. Reusability of membranes

The reusability of fabricated membrane was tested by conducting membrane permeation experiments for 30 cycles using the same membrane permeation set up as shown in Fig. 3. Each cycle was carried out under optimum condition of flow rate: 23 mL.min^{-1} and temperature: 25 °C. The concentration of feed solution was maintained as 1.5 mmol. L^{-1} and each cycle was operated continuously for 8 h of operation time.

2.2.7. MWCO of the membrane

The membrane based permeation experiment was conducted to determine the Molecular Weight Cut-off (MWCO) value of prepared TFN membranes. The experiments were performed in flat sheet TFN membranes having an active surface area of 18.32 cm^2 under room temperature. The feed solution of PEG with molecular weights ranging from 100 Da to 250 Da was used in this experiment. Every feed solution was prepared in a concentration of 1 g.L^{-1}. The MWCO is defined as the molecular weight of PEG with rejection of 90% on the membrane.

3. Results and discussion

3.1. Characterization of functionalized organoclay

The characterization of raw and functionalized clay was carried out through different characterization techniques. The FTIR spectra of raw bentonite and functionalized bentonite was compared as shown in Fig. S1, which confirms that the functionalized clay contains functional groups C-C, C=C where vibrational frequency was obtained at 1490 cm^{-1} and 1580 cm^{-1} respectively. The presence of N-O was obtained at vibrational frequency of 1250 cm^{-1}. The presence of additional functional groups on functionalized clay confirms the functionalization of raw bentonite. XPS analysis of functionalized clay contain C-N-C and N-O bond which exhibited binding energy shift at 401.5 eV and 400 eV (Fig. S2). This confirms the introduction of IL into

clay. TGA representation of raw bentonite and functionalized clay revealed the higher thermal stability of IL-clay upto 650 °C as shown in Fig. S3, whereas thermal stability of clay was obtained at temperature of 480 °C. The surface morphology of bentonite and IL-bentonite were compared, where IL-clay shows exfoliation of stacked layer of clay. Furthermore, the EDX analysis reveals the presence of N in IL-clay as shown in Fig. S4. TEM and BET analysis of raw bentonite and IL-modified organoclay are shown in Fig. S5 and S6.

3.2. Characterization of organoclay based nanocomposite membranes

The FTIR spectra and characteristic absorption peak of three TFN membranes were interpreted and compared with the raw PSf membrane as depicted in Fig. S7. The spectra represented the polyamide bond formation in TFN membrane by the interfacial interaction between aliphatic and aromatic monomers. The M_{FBn2} exhibited a substantial absorption peak at 1610 cm^{-1} due to C═O vibration at polymer interface, whereas the raw polymeric support does not exhibit characteristics vibration at this region. In M_{FBn1} and M_{FBn3} membranes, these peaks appeared at a very low resolution, wherein in the case of M_{FBn1} the narrow and weaker intensity of this peak would not be sufficient to indicate the C═O vibration. Additional sharp and intensified peaks were found at 1398 cm^{-1}, which is assigned to the typical vibration of C-N bond; this vibrational peak is more prominent in the case of M_{FBn2} and M_{FBn3}, where the raw PSf has exhibited no stretching vibration [26]. The peak at 1600 cm^{-1} has marked aromatic C═C of IL of polymeric composite. This peak is highly intense in the case of M_{FBn2}. Highly intense in-plane vibration of C-C and C═C in M_{FBn2} portrayed the effective growth of amide linkage due to the introduction of 0.4 wt% of IL added organoclay into the aqueous media of polymeric reaction. The driving force behind the better polymerization reaction is reactive amide linkage which is adjacent to the aromatic counterpart of IL, where electronic delocalization over the imidazolium group can give stabilization in addition to the MPD monomer [27].

XPS analysis was used to determine the elemental composition of support and TFN membranes and this is shown in Fig. 4. The chemical composition of TFN membranes was evaluated following their corresponding binding energy values. A quantitative analysis was also performed to estimate the characteristics peaks through resolving their broad peak area. The C1s and O1s scan of raw PSf support is shown in Fig. 4(A.1) and Fig. 4(A.2) respectively, which correspond to the binding energy shift of C-C, C-O and C-S respectively, whereas Fig. 4(B.1) and Fig. 4(B.2) represent the C1s scan and O1s scan of bentonite modified PSf, which shows the presence of an additional peak due to the binding energy shift of O-H in Fig. 4(B.2). The C1s scan of M_{FBn1} served as a broad peak, which can be resolved into distinct peaks, including the bonding with a different heteroatom. The peak at 289 eV is assigned to the typical C═O of the amide linkage, whereas the amidation reaction can also be ascribed from the binding energy of C-N at 284.3 eV. The increase in the intensity of the C-N bond has carried out the loading of IL-clay to fabricate the amide linkage suitably. Another peak at 284.8 eV corresponds to the hydrophobic alkyl linkage in aromatic/aliphatic polymer composite [28]. In the N1s scan, the major peaks are ascribed to the N-H of the amide linkage. In contrast, the minor contribution can also be achieved from the N-O interaction within the inner hydroxyl and aromatic amine monomer.

The XPS of M_{FBn2} and M_{FBn3} also appraised the binding energy splitting of C1s, N1s and O1s scans. In addition to the better performance of IL within clay sheets, the M_{FBn2} possessed high intensity in the resolving peak of C-N at 287.3 eV. The additional peak at C═O in both the membranes can be attributed to an amide layer over PSf support. The presence of C═O peak in M_{FBn3} has pointed out the significant interaction of MPD monomer with the imidazolium fragment through successive pi-pi interaction, van der Waal interaction and interaction of hydrophobic alkyl linkage with reactive amide platform [29]. Therefore, the percentage elemental composition of the three membranes was

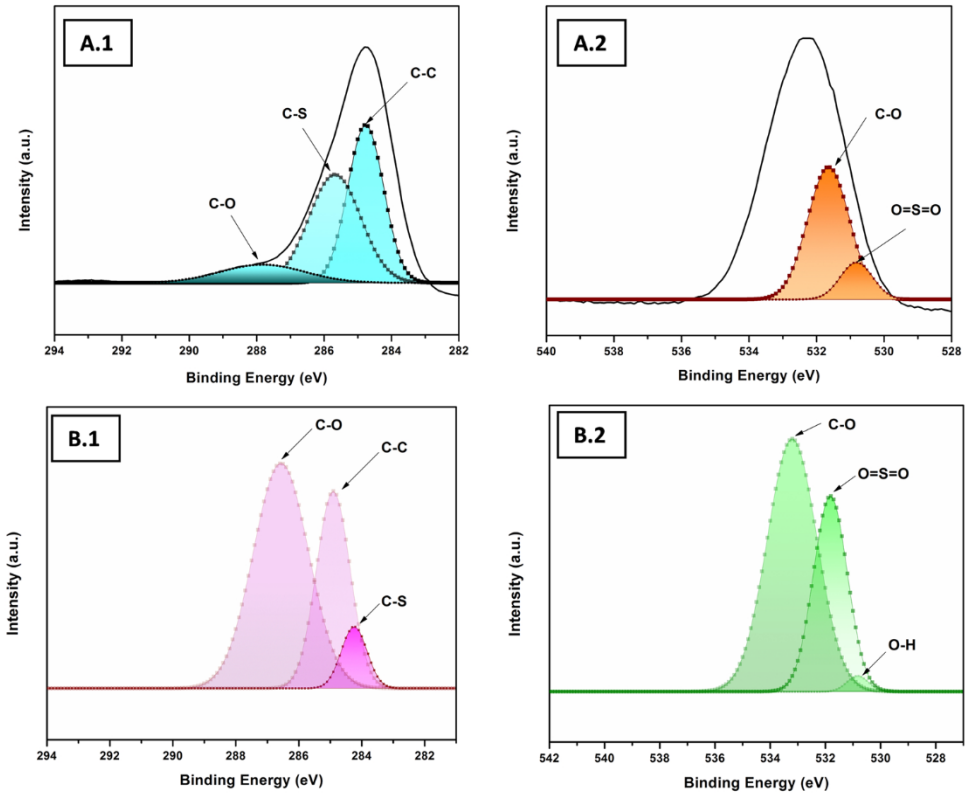

Fig. 4. XPS spectra of (A) M_{PSf} (B) M_{Bn}(C) M_{FBn1} (D) M_{FBn2} and (E) M_{FBn3} membranes (A.1, B.1, C.1, D.1, E.1) C1s; (A.2, B.2, C.3, D.3, E.3) O1s; (C.2, D.2, E.2) N1s high resolution scan and (F) Survey scan spectra of M_{PSf}, M_{Bn}, M_{FBn1}, M_{FBn2} and M_{FBn3} membranes.

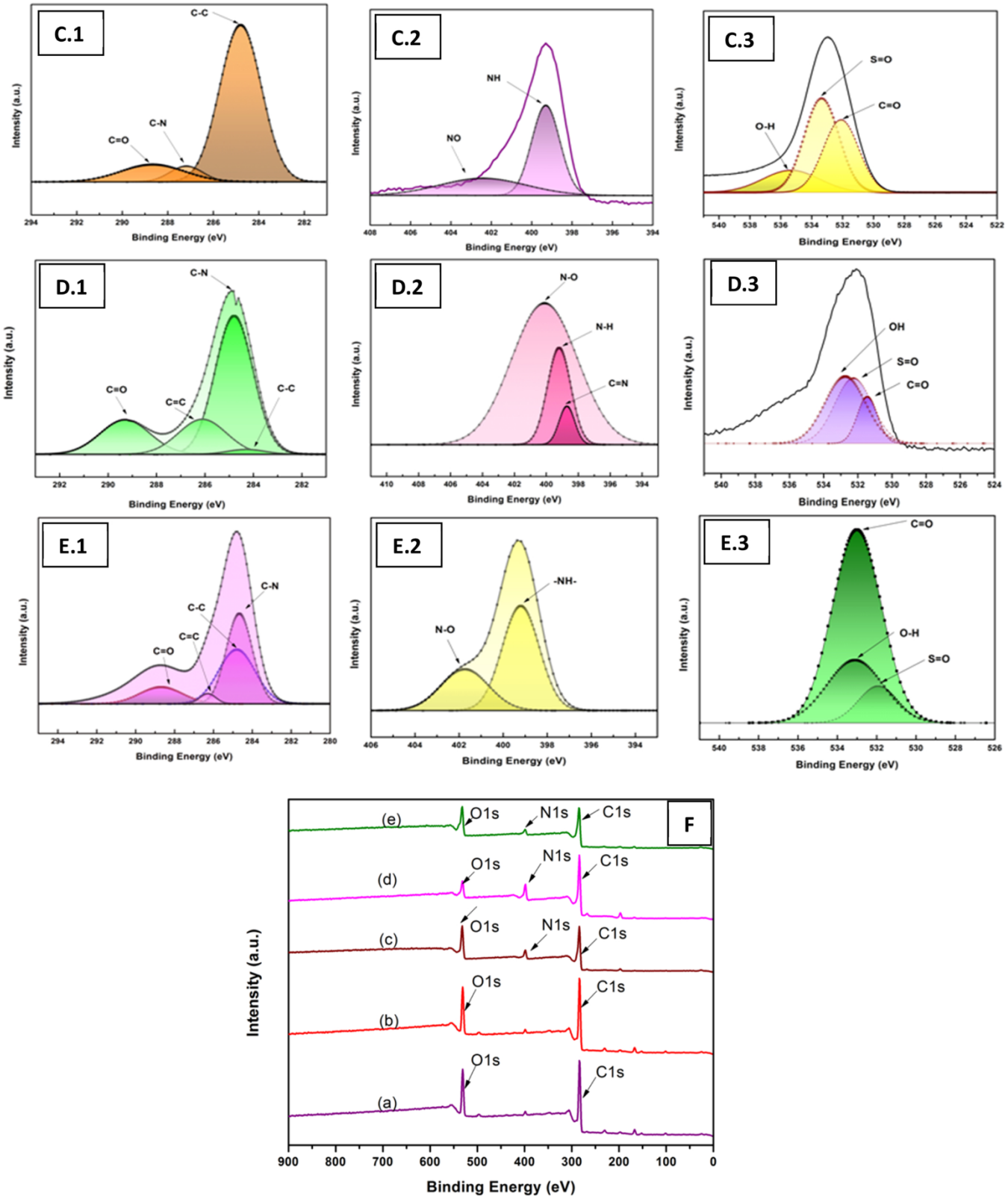

Fig. 4. (*continued*).

discussed with reference to their survey spectrum.

The thermal behavior of clay-[1-hexyl-3-methylimidazolium chloride] based composite membranes was analyzed under N_2 atmosphere and the stability performance was observed through two step degradation, as shown in Fig. S8. Therefore, thermal stability was noticeably observed for PSf membrane and IL-clay composite membranes of M_{FBn1}, M_{FBn2} and M_{FBn3}. The thermal degradation temperature for PSf membrane was observed as 145 °C, where the gradual increase of degradation temperature suggested a systematic integration of clay sheets and the structural deformation of polymeric cleavage over membrane

support. Therefore, the M_{FBn2} exhibited a higher degree of decomposition temperature due to the strong amide linkage attached to the phenyl ring, which can undergo an effective pi-pi stacking with the imidazolium group of IL, introduced within clay sheets. The maximum decomposition temperature was obtained as 493 °C, 511 °C, 515 °C and 502 °C for M_{PSf}, M_{FBn1}, M_{FBn2} and M_{FBn3} membranes respectively. The highest degradation temperature and lowest weight percent loss were estimated for $M_{FBn2.}$ The weight loss of other membranes was gradually decreased with reference to the temperature and found to be a function of IL-clay content. Therefore, the greater degree of thermal stability can be attributed to the –CONH-, the backbone of the polymeric interface. This polymeric linkage has gained more vital strength due to the aromatic ring current of the imidazolium group.

The surface morphology of clay-[1-hexyl-3-methylimidazolium chloride] added TFN membranes were characterized and compared to the pristine TFC membrane seen in Fig. 5. The surface feature of M_{FBn1} and M_{FBn3} membranes appeared to have visible "leaf-like folds" produced due to the dispersion of IL grafted bentonite in an organic solvent. The introduction of IL-clay into the MPD monomer could result in swelling properties through the adsorption of water molecules within their void area. During polymerization at the inter phase of two immiscible solvents, the hydration of organic solvent can be alleviated by driving water molecules from the aqueous to the organic phase. Therefore, the release of hydration energy could increase faster the diamine diffusion towards the region of interfacial polymerization, which can increase the width of the reaction zone leading to the characteristic appearance of ridge and valley morphology throughout the cross sectional portions. In the case of M_{FBn2}, the ridge and valley structure appear in high resolution and the polymerization reaction can proceed symmetrically with a homogeneous distribution of morphological deviation [23]. The driving force of this observation can be ascribed from the diffusion rate of diamine due to the difference in interfacial tension which increases with an increase in the percentage of IL in M_{FBn2} and, therefore, the propagating nature of polycondensation have grown across the separation barrier.

The surface morphology of TFN membranes has evaluated the porous characteristics of the prepared composite membrane. The M_{FBn2} possesses a polymeric active site on the membrane surface indicated by the cylindrical shaped morphology, as shown in Fig. 5. The distribution of pores was also homogenous with reference to the polymeric groups [29]. The membrane M_{FBn1} showed agglomeration of functionalized bentonite and more pore blocking. In $M_{FBn3,}$ with an increase in % of IL-clay, a large number of IL-clay are accumulated into their surface, which may prevent the passage of water molecules by blocking the membrane pores. Therefore, we could not observe the proper ridge and valley morphology in the cross sectional part of M_{FBn3}.

The exterior surface roughness of TFN membrane was determined by AFM characterization done in the tapping mode. Fig. 6 depicts the surface roughness of M_{PSf}, M_{FBn1}, M_{FBn2} and M_{FBn3} respectively. The average roughness (R_a) is 11.80 nm, 15.67 nm, 25.235 nm and 21.867 nm for M_{PSf}, M_{FBn1}, M_{FBn2} and M_{FBn3} respectively. Thus, it indicates that the IP mediated polyamide layer can unusually improve the roughness of prepared TFN membranes; with the increment in the roughness of wt% of clay-[1-hexyl-3-methylimidazolium chloride] framework, the effective surface area for mass transfer increases which thereby increases the mass transfer flux.

In a nut shell, the effective performance of the developed membrane is a result of the successful interfacial polymerization process between the two monomers in a definite proportion. MPD is an organic compound containing two amine groups, which may act as an efficient monomer to form a mechanically strong polymer composite. The two amine groups of MPD monomer have a high affinity towards forming an amide bond with another monomer of adipoyl chloride. Since there is a strong hydrogen bonding of –NH- group of MPD with water molecules in aqueous phase. Therefore, the high solubility of MPD monomer in the aqueous phase is also considerable. Although this type of monomer is used for RO membrane to separate or fractionate large molecules like dye molecules, this will be highly effective enough to separate the polyphenol molecules with a molecular weight of 458.372 g/mol.

Adipoyl chloride is an organic compound having two acyl groups. These groups are highly reactive towards the affinity of the nucleophile. The long alkyl chain of adipoyl chloride will act as an effective support medium to form a high thermal stability polymer composite. The addition of adipoyl chloride to MPD will exhibit a polymerization reaction at the extent of a high rate. One of the most challenging properties of adipoyl chloride is that it will form an aliphatic/aromatic polymer, which gets high thermal stability at a relatively low temperature compared to TMC. In the case of TMC, the polymer formed will not be superior enough to exhibit better thermal stability in the presence of functionalized clay. The aliphatic/aromatic polyamide layer will not be sterically overcrowded to react with the polyphenol molecule, as the molecule contains more than two aromatic rings. Since polyphenol molecule is bulkier in size, therefore during separation performance; the molecule will experience steric effect predominantly compared to intermolecular attractions.

The bentonite clay is incorporated into the polyamide layer to increase the surface area of the reaction zone. The polymerization reaction will be effectively occurred to form a thermally stable polyamide layer. The polyamide layer formed within the exfoliated clay sheets will be supported by the layers of functionalized clay, which also propitiously give a suitable reaction zone to exhibit intermolecular attraction with polyphenol molecules.

3.3. Selectivity of M_{FBn2} for the removal of EGCG

Thin film functionalized clay based membranes were prepared through the formation of polyamide layers by interfacial polymerization. These membranes were designed to study their effective behavior towards tea catechin molecules. The surface of these membranes was loaded with chemically active –CONH- fragments, which possess strong intermolecular hydrogen bonding with number of hydroxyl groups of epigallocatechin gallate ($C_{22}H_{18}O_{11}$).

The selectivity of membrane is compared for removal of tea polyphenols viz. epicatechin (EC), epigallocatechin (EGC), gallocatechin gallate (GCG), epicatechin gallate (ECG) and epigallocatechin gallate (EGCG). The rejection efficiency of M_{FBn2} possessed the following order EC<EGC<ECG<GCG<EGCG. The rejection % of EC is 65%, whereas, the rejection % of EGC, ECG and GCG is 71.45%, 76% and 80.35% respectively. The highest rejection is exhibited by the tea polyphenol EGCG, which is obtained as 94%. EC molecule contains two hydroxyl groups at the adjacent carbon of benzene ring experiences less hydrogen bonding interaction compared to the EGC, which contains three adjacent hydroxyl groups. The polyphenol containing gallate group possess stronger interaction with the –CONH- linkage due to the increase in hydroxyl groups. The electron deficient carbonyl of gallate groups have tendency to feel interaction with the available nonbonding pair of –CONH- group. The highest rejection behavior of membrane is observed in case of EGCG; this may be due to the greater size of molecule and increase in hydrogen bonding with –CONH- group. (Fig. 7).

3.4. Performance of TFN membrane for separation of EGCG

The thermodynamic behavior of membrane based separation technique was explained in terms of time (h), feed concentration ($mmolL^{-1}$) and transmembrane pressure (bar). The consequence effect of permeation time on the separation of EGCG from its aqueous solution in terms of flux and % rejection is shown in Fig. 8(A.1) and Fig. 8(A.2) respectively, which clearly showed that the membrane flux decreases progressively with an increase in permeation time. Nevertheless, the hierarchical deposition of amide interconnection of two monomer fragments is expected to possess more susceptible cohesive forces like hydrogen bonding and van der Waal interaction for polyhydroxy EGCG

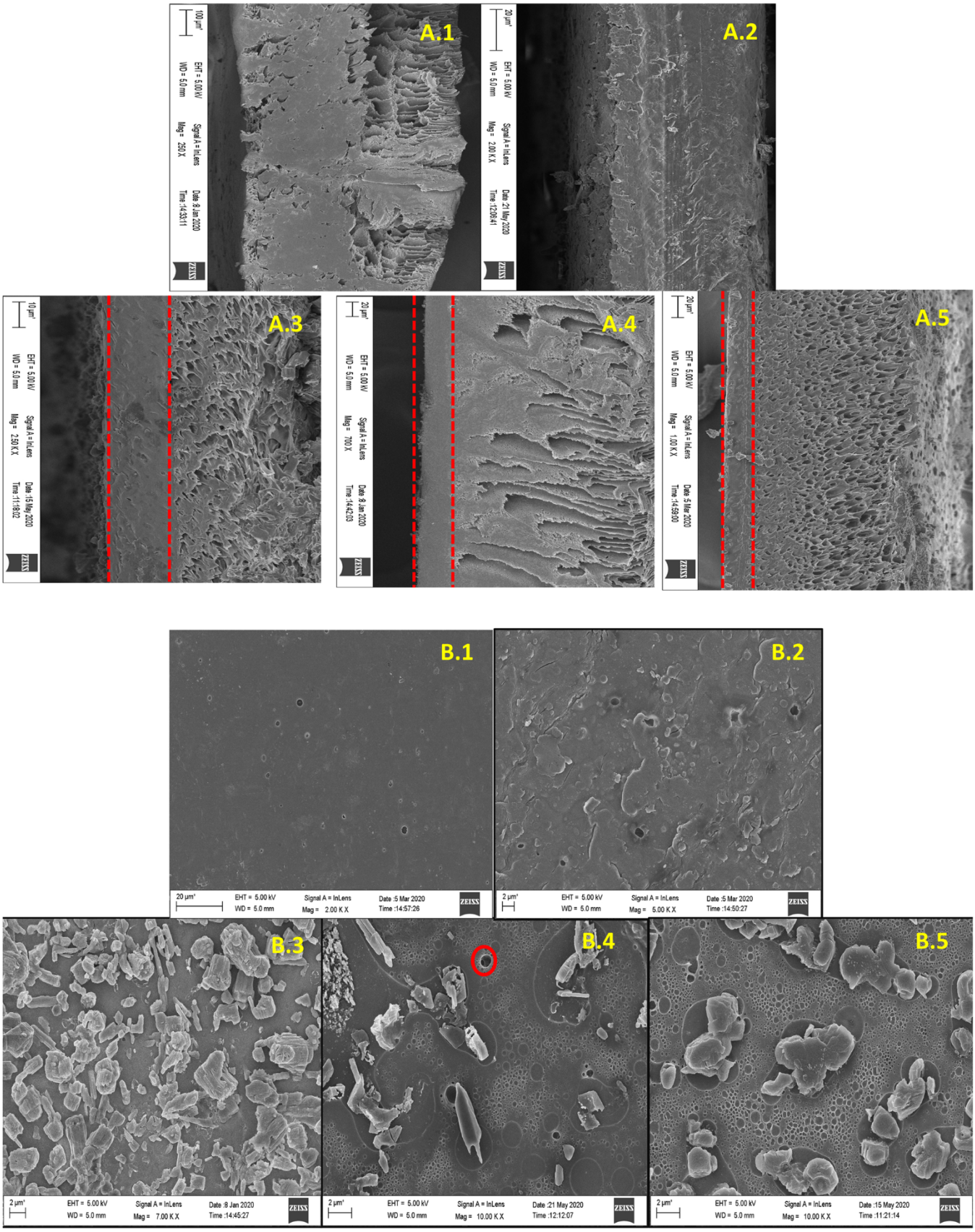

Fig. 5. : FESEM images (A.1-A.5) Cross sectional view; (B.1-B.5) Surface morphology; of (a) M_{PSf} (b) M_{Bn} (c) M_{FBn1}(d) M_{FBn2} and (e) M_{FBn3} membranes.

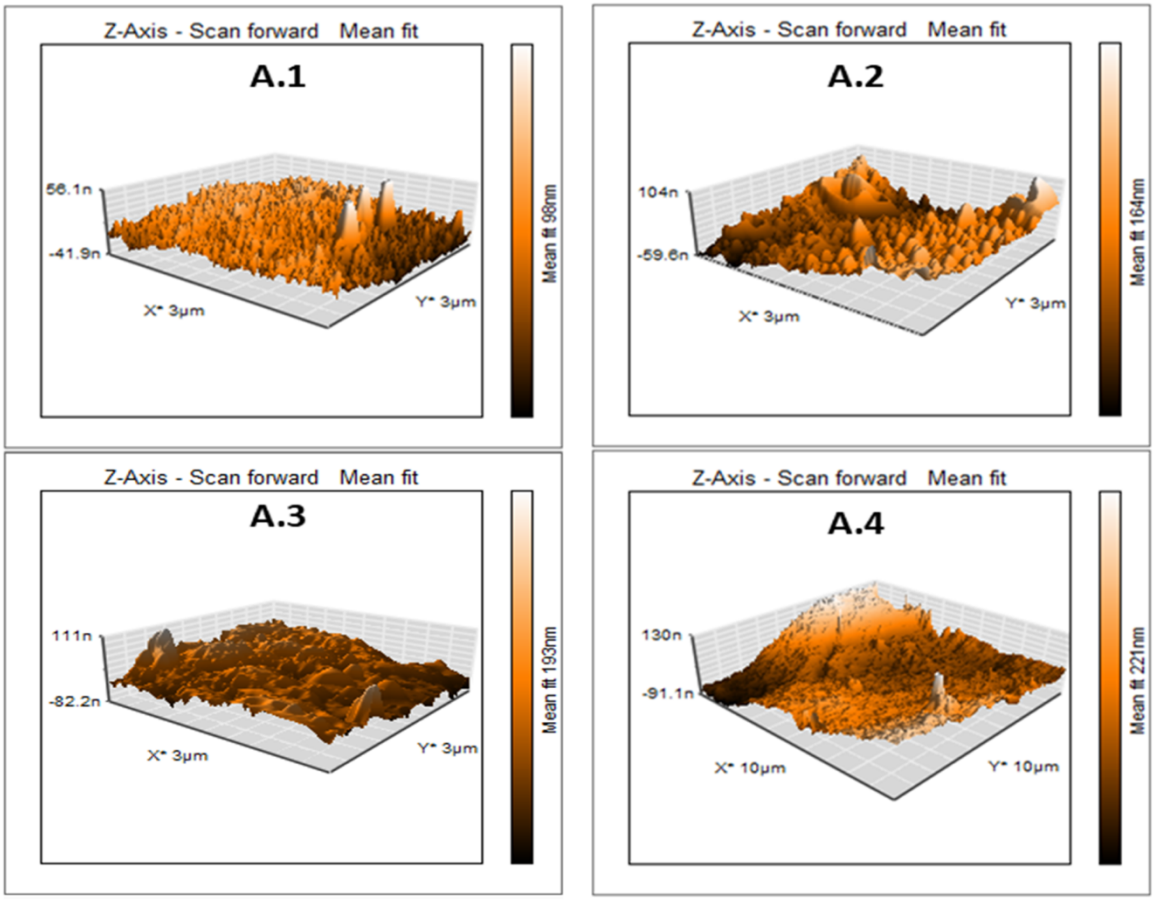

Fig. 6. : AFM images of (A.1) M_{PSf} (A.2) M_{FBn1} (A.3) M_{FBn2} and (A.4) M_{FBn3} membrane.

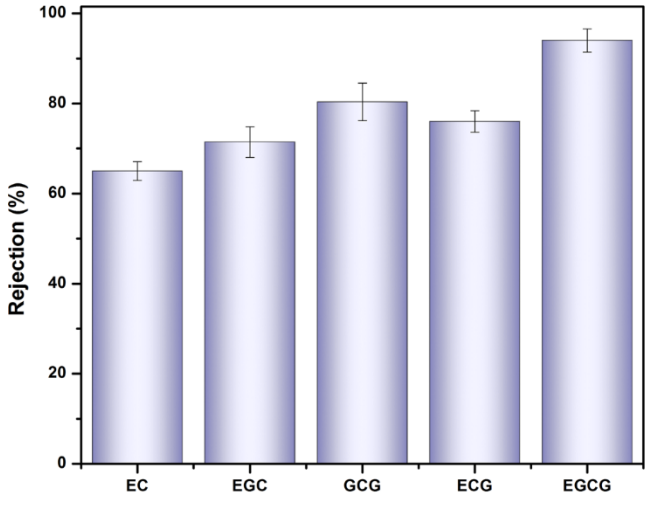

Fig. 7. Selective performance of M_{FBn2} membrane.

molecule and thereby implicated the multi-channel passage towards water flow through the membrane. Multi-channel passages are developed due to the fabrication of amide layer over membrane surface, which explored finger like projections with macrovoids, which will act as suitable pathway to allow the passage of water molecules.

The higher porosity response of the membrane surface could be effective due to the macroscopic organoclay, which can play an essential role in increasing the water permeability. The steep decrease in flux value explains the time dependent behavior of membrane fluxes, which portrayed the negative variation of flux value with time. Therefore, after each one hour of absorbance reading, the flux value decreases and minimum at 36.73 $L.m^{-2}.h^{-1}$ in support polymeric membrane. It is seen that slightly better value could be found at 45.78 $L.m^{-2}.h^{-1}$ in the case of M_{FBn2}. With a one hour interval of time, the diffusivity rate continuously decreases due to the hydraulic resistance added to the permeate flux as shown in Fig. 8(A.1).

It is worth mentioning that the higher rejection ratio of EGCG molecule was achieved in the case of M_{FBn2}, due to the basic component of membrane surface free energy, whose steady increase could be surprisingly derived from the reinforcing interaction of EGCG molecule through their arbitrarily arranged hydroxyl group with –CONH- moiety of an amide bond. The excellent rejection value for M_{FBn2} is due to the synergy between hydrophilicity and stabilized aromatic ring current of diazole fragment induced by the integration of IL molecule within stacked clay sheets.

The performance of polyphenol separation under pressure variation is essential to produce consistent water flux and pure rejection ratio of EGCG molecules. This can be defined as a hydrostatic pressure gradient across the sides of the membrane. When transmembrane pressure increases during membrane permeation, the solute molecules were partly retained and accumulated over the membrane surface due to the decrease in the convective flow of the feed stream. Superlative reduction of solute concentration towards permeates side (C_p) compared to within the bulk of surface may be the cause for declining flux value. The process of mass accumulation on the boundary layer of the reactive amide layer undergoes concentration polarization (C_p). In Fig. 8(B.1) and 8(B.2), effect of transmembrane pressure on flux and % rejection was reported. The rejection efficiency of membranes was assessed as 83.93% in M_{PSf}, whereas M_{FBn1} and M_{FBn3} have shown the percentile rejection efficiency

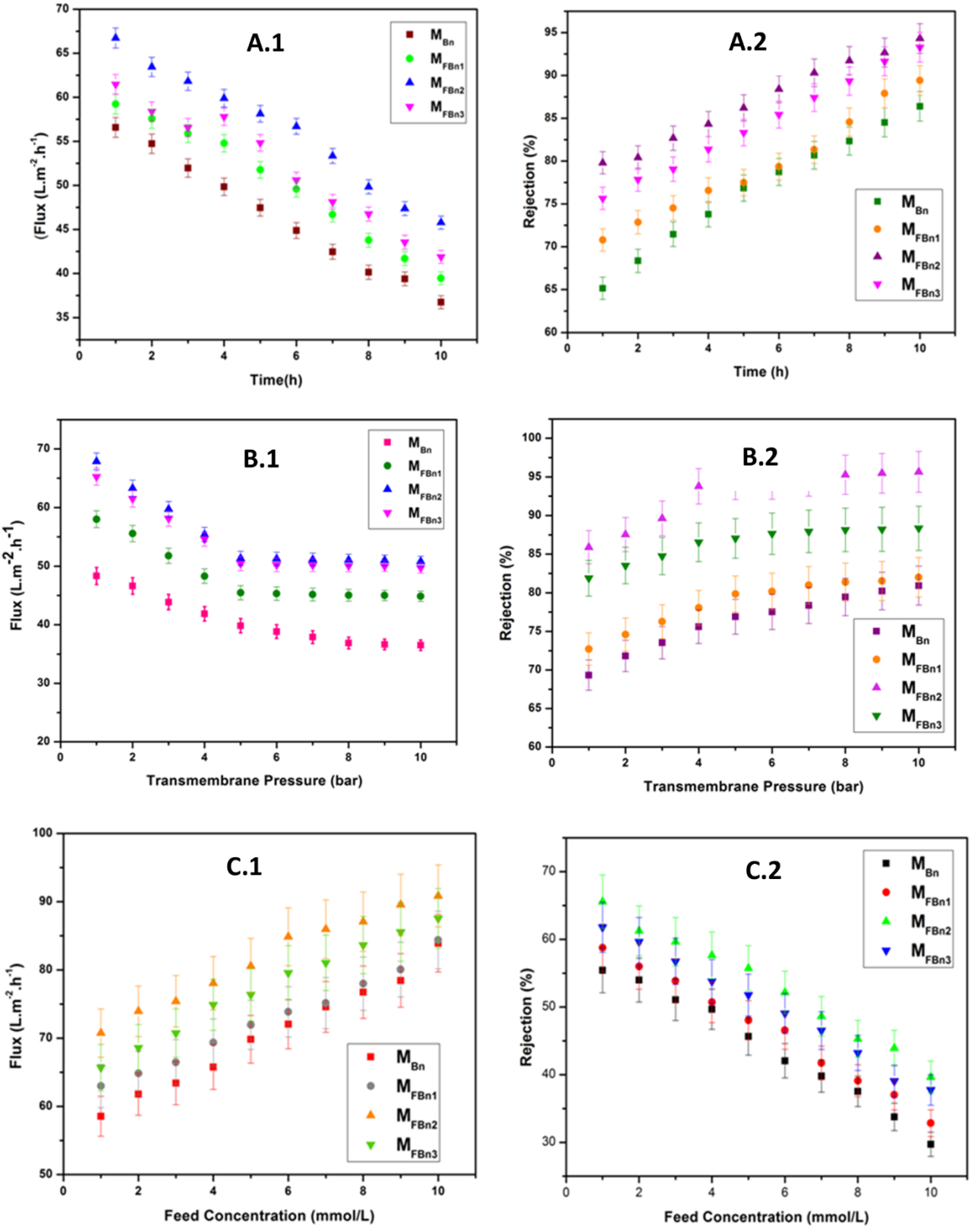

Fig. 8. (A.1): Time dependent behavior of membrane flux, (A.2): Rejection for M_{Bn}, M_{FBn1}, M_{FBn2} and M_{FBn3} respectively with time, at feed concentration: 1.5 mmol. L^{-1}, flow rate: 23 mL.min^{-1}, transmembrane pressure: 5 bar, temperature: 25 °C;(B.1): Transmembrane pressure dependent behavior of membrane flux, (B.2): Rejection by M_{PSf}, M_{FBn1}, M_{FBn2} and M_{FBn3} respectively with transmembrane pressure, where feed concentration: 1.5 mmol.L^{-1}, flow rate: 23 mL.min^{-1} and temperature: 25 °C;C.1: Feed concentration dependent behavior of membrane flux, (C.2): Rejection by M_{PSf}, M_{FBn1}, M_{FBn2} and M_{FBn3} respectively with feed concentration, where transmembrane pressure: 5 bar, flow rate: 23 mL.min^{-1} and temperature: 25 °C.

at 85.01 and 87.9, respectively. The pressure driven polarization effect could be significantly observed in case of M_{FBn2}, where the 0.4 wt% of clay-[1-hexyl-3-methylimidazolium chloride] incorporated TFN membrane showed 94% rejection because the polarizing power of positively charged nitrogen atom brings to bear the more significant attraction with the polyhydroxy group available in the EGCG molecule. Furthermore, the delaminated clay sheets have resulted in interlaced porous structures, which can diffuse the rejected molecule back to the membrane surface.

To study the effect of feed concentration ranges from 1 mmol/L to 10 mmol/L on the membrane performance during the separation of EGCG, experiments were conducted with different concentrations of feed solution at constant operational temperature and pressure, and the effects on flux and %rejection are shown in Fig. 8(C.1) and Fig. 8(C.2) respectively. It puts forward that the transfer of mass solute through the prepared membranes was controlled by the diffusivity rate of the feed solution, where the diffusion of particulate or molecule to the membrane internal surface increases with an increase in concentration. Meanwhile, the available reactive surface area of the membrane was gradually occupied by particulate feed solution and achieved a point of saturation after completely enveloping the surface. The flux value increases in the case of M_{FBn2} upto 90.84 $L.m^{-2}.h^{-1}$, due to the increase in diffusion via concentration gradient, which allows the substantial interaction of EGCG through intermolecular hydrogen bonding with amide linkage resulting from condensation polymerization. In the case of M_{FBn1} and M_{FBn3}, the introduction of organic filler could not give sufficient mechanical strength to exfoliate the clay sheets; therefore, the membrane porosity becomes perturbed and permeability decreases. The concentration dependent variation of membrane flux and rejection can also be explained according to the concentration polarization process [30–32]. It generally refers to the emergence of concentration gradient across membrane surface due to accumulation of molecules over membrane surface. With increase in concentration, there is a probability of accumulation of EGCG over membrane surface through hydrogen bonding interaction, which increase the membrane flux through membrane pores and decreases the rejection of molecule with more or less steric factor. The concentration of transported species increases on permeates side and feed stream may feel size dependent steric crowding and may not be efficient for rejection of polyphenols.

3.5. Antifouling behavior of thin film nanocomposite membranes

Membrane fouling is the property of membranes that can hinders the applications of membranes in different separation processes. The fouling properties of membrane increase the operational cost of the membrane. Therefore, fouling resistance ability is crucial to NF membrane applications [33].

Membrane antifouling characteristics can be determined using flux recovery ratio (FRR), which can determine the permeate flux after repeated permeation experiments. A model protein, bovine serum albumin (BSA), was used to determine the antifouling behavior of prepared TFN membranes. Therefore, an aqueous solution of BSA was prepared at a concentration of 1 $g.L^{-1}$ and used for three flux cycles. These three flux cycles were DI water flux, flux with BSA as the feed and water flux of back flushing the membrane for 45 min in 1 × phosphate-buffered salines (PBS). The fouling resistance power of membranes was determined in terms of FRR, irreversible flux decline ratio (IFR), and relative fouled flux ratio (RFR), as shown in the following equations [33]. It is found that the better antifouling characteristics are shown by the membrane having higher and lower FRR and IFR, respectively.

$$FRR(\%) = \frac{J_P}{J_W} \times 100 \quad (1)$$

$$IFR(\%) = 100\text{–}FRR \quad (2)$$

$$RFR(\%) = \frac{J_B}{J_W} \times 100 \quad (3)$$

Where, J_W is the pure water flux, J_P is the water flux after black flushing and J_B is BSA solution flux respectively.

The FRR of M_{FBn2} membrane is 81%, whereas, for pure PSf membrane, it is obtained as 41%. The higher FRR of the modified membrane can be drawn from electrostatic repulsion between BSA and the negative M_{FBn2} membrane. In spite of having better antifouling characteristics of membrane, as presented data in Fig. 8(A.1) showed the comparative decrease of membrane flux with increase in time period. This may be due to the interaction of tea polyphenol with amide linkage with increase in time. It may slightly effect on the effective passage of water molecules through membrane pores. The diffusion rates of molecules through membrane pores are controlled by the continuous flow of feed solution. As the prepared membrane contain functionalized porous nanofiller. This act as also a driving force to impart the antifouling characterizes more to the membrane surface. There is no possibility for molecules to deposit over membrane surface, as the presence of highly reactive amide linkage allows strong inter molecular attractions. (Fig. 9).

3.6. Reusability and long term used of TFN membrane

The reusability of membranes is essential from an industrial point of view. Our previous study reported the membrane stability for three months, where it was established that flux and rejection remain almost the same for this period [34]. Depending upon the membrane flux results, the prepared three membranes were selected for the reusability study during 30 continuous filtration cycles. Each cycle involved the determination of membrane flux through continuous 8 h of membrane permeation experiment. It was seen that, the membrane flux obtained from each cycle remain almost same. The membrane flux was obtained as 49.83 $Lm^{-2}h^{-1}$ for one continuous cycle under transmembrane pressure of 5 bar, time 8 h and flow rate 23 $mL.min^{-1}$, effective membrane surface area 18.32 cm^2 was treated in each cycle. The flux value decreases to 49.76 $Lm^{-2}h^{-1}$ in the next complete cycle. Therefore, these membranes can be efficiently used in cyclic filtration with negligible reduction of membrane flux. The reusability of membranes can be determined as approximately 99%.

The flux was calculated for the period of 6 months and it was observed that, the flux value was slightly declined due to the compaction of membranes at 4 months. From Fig. S14 (given in supplementary

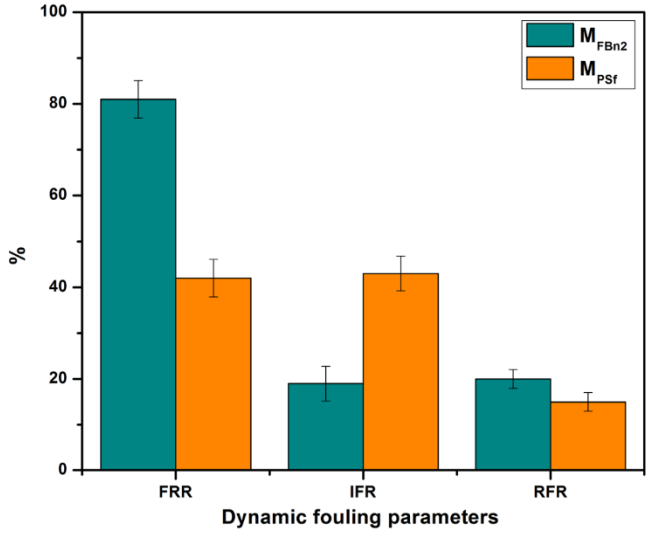

Fig. 9. Dynamic fouling studies of M_{PSf} and M_{FBn2} membranes.

material) it is seen that, the separation performance was kept at a high level after a long period of work. Prior to filtration, the membranes were washed using deionised water for ensuring the maximum selectivity and flux.

4. Conclusion

Selective separation of epigallocatechin gallate was studied in this work. Clay based nanomaterial was developed using ionic liquid [1-hexyl-3-methylimidazolium chloride] to exfoliate the stacked clay sheets. This clay-[1-hexyl-3-methylimidazolium chloride] framework was introduced as a nano additive in the TFN membrane to increase the antifouling properties and selective separation of epigallocatechin gallate. TFN membranes were prepared using different wt% of clay-[1-hexyl-3-methylimidazolium chloride] and detailed characterization was performed to give an insight on membrane properties. M_{FBn2} membrane having 0.4 wt% of functionalized clay exhibited better rejection efficiency for EGCG. This membrane possesses contact angle of 53.3° and it was stable up to 515 °C. The membrane surface roughness was obtained at 25.235 nm. A polyamide layer (-CONH-) was fabricated over polymeric support through interfacial polymerization. Detail study on selective separation of epigallocatechin gallate in aqueous media was performed using a highly efficient antifouling thin film nanocomposite membrane. It was observed that the formation of the polyamide layer boosts the separation process for EGCG and proliferate potential applications of the membrane in the separation process. It was also observed that the parameters such as concentration, pressure and time act as significant role that inevitably decreases the membrane flux and consequently increase rejection efficiency. Higher rejection of 94% EGCG was observed in case of M_{FBn2}, which include feed concentration of 1.5 $mmolL^{-1}$, flow rate 23 $mL.min^{-1}$ and transmembrane pressure of 5 bar. Based on this, we have investigated the inter related dynamic mechanism of membrane flux, rejection efficiency and membrane fouling behavior during membrane permeation experiments.

CRediT authorship contribution statement

Alimpia Borah: Methodology, Software, Formal analysis, Investigation, Resources, Data curation, Writing – original draft, Writing – review & editing. **Monti Gogoi**: Formal analysis, Investigation, Resources, Data curation, Writing – original draft. **Rajiv Goswami**: Software, Writing – original draft. **Hrishikesh Sarmah:** Methodology, Investigation. **Krishna Kamal Hazarika:** Methodology**. Swapnali. Hazarika**: Conceptualization, Visualization, Methodology, Validation, Writing – review & editing, Supervision, Project administration, Funding acquisition.

Declaration of Competing Interest

The authors declare that they have no known competing financial interests or personal relationships that could have appeared to influence the work reported in this paper.

Acknowledgments

The authors gratefully acknowledge Council of Scientific & Industrial Research (CSIR), New Delhi, India for research grant MLP-1018 and Dr G Narahari Sastry, Director, CSIR-NEIST for encouraging the research group to carry on this work.

Appendix A. Supporting information

Supplementary data associated with this article can be found in the online version at doi:10.1016/j.jece.2022.107423.

References

[1] Q. Meng, S. Li, J. Huang, C. Wei, X. Wan, S. Sang, C. Ho, Importance of the nucleophilic property of tea polyphenols, J. Agric. Food Chem. 67 (2019) 5379–5383.
[2] M.S.M. Mansour, H.I. Abdel-Shafy, F.M.S. Mehaya, Valorization of food solid waste by recovery of polyphenols using hybrid molecular imprinted membrane, J. Environ. Chem. Eng. 6 (2018) 4160–4170.
[3] L. Xing, H. Zhang, R. Qi, R. Tsao, Y. Mine, Recent advances in the understanding of the health benefits and molecular mechanisms associated with green tea polyphenols, J. Agric. Food Chem. 67 (2019) 1029–1043.
[4] S. Liang, F. Wang, J. Chen, D. Granato, L. Li, J.F. Yin, Y.Q. Xu, Optimization of a tannase-assisted process for obtaining teas rich in theaflavins from Camelia sinensis leaves, Food Chem. X 13 (2022), 100203.
[5] A. Sood, M. Gupta, Extraction process optimization for bioactive compounds in pomegranate peel, Food Biosci. 12 (2015) 100–106.
[6] J. Zivkovic, K. Savikin, T. Jankovic, N. Cujic, N. Menkovic, Optimization of ultrasound-assisted extraction of polyphenolic compounds from pomegranate peel using response surface methodology, Sep. Purif. Technol. 194 (2018) 40–47.
[7] X. Luo, J. Cui, H. Zhang, Y. Duan, D. Zhang, M. Cai, G. Chen, Ultrasound assisted extraction of polyphenolic compounds from red sorghum (Sorghum bicolor L.) bran and their biological activities and polyphenolic compositions, Ind. Crops Prod. 112 (2018) 296–304.
[8] A. Kumar, B.K. Thakur, S. De, Selective extraction of (−)epigallocatechin gallate from green tea leaves using two-stage infusion coupled with membrane separation, Food Bioprocess Technol. 5 (2012) 2568–2577.
[9] M.S. Manna, P. Saha, A.K. Ghoshal, Separation of medicinal catechins from tea leaves (Camellia sinensis) extract using hollow fiber supported liquid membrane (HF-SLM) module, J. Membr. Sci. 471 (2014) 219–226.
[10] A. Giacobbo, A.M. Bernardes, M.N. de Pinho, Sequential pressure-driven membrane operations to recover and fractionate polyphenols and polysaccharides from second racking wine lees, Sep. Purif. Technol. 173 (2017) 49–54.
[11] C. Conidi, A. Cassano, F. Caiazzo, E. Drioli, Separation and purification of phenolic compounds from pomegranate juice by ultrafiltration and nanofiltration membranes, J. Food Eng. 195 (2017) 1–13.
[12] C. Zhang, J. Xue, X. Yang, Y. Ke, R. Ou, Y. Wang, S.A. Madbouly, Q. Wang, From plant phenols to novel bio-based polymers, Prog. Polym. Sci. 125 (2022), 101473.
[13] Y. Lu, Z. Wang, W. Fang, Y. Zhu, Y. Zhang, J. Jin, Polyamide thin films grown on PD/SWCNT-interlayered-PTFE microfiltration membranes for high-permeance organic solvent nanofiltration, Ind. Eng. Chem. Res. 59 (2020) 22533–22540.
[14] F. Zhang, J. Fan, S. Wang, Interfacial polymerization: from chemistry to functional materials, Angew. Chem. Int. Ed. Engl. 59 (2020) 21840–21856.
[15] L. Paseta, C. Echaide-Gorriz, C. Tellez, J. Coronas, Vapor phase interfacial polymerization: a method to synthesize thin film composite membranes without using organic solvents, Green Chem. 23 (2021) 2449–2456.
[16] Y. Song, J. Fan, S. Wang, Recent progress in interfacial polymerization, Mater. Chem. Front. 1 (2017) 1028–1040.
[17] W. Choi, J.E. Gu, S.H. Park, S. Kim, J. Bang, K.Y. Baek, B. Park, J.S. Lee, E.P. Chan, J.H. Lee, Tailor-made polyamide membranes for water desalination, ACS Nano 9 (2015) 345–355.
[18] X. Yang, Controllable interfacial polymerization for nanofiltration membrane performance, improvement by the polyphenol interlayer, ACS Omega 49 (2019) 13824–13833.
[19] J. Bai, W. Lai, L. Gong, L. Xiao, G. Wang, L. Shan, S. Luo, Ionic liquid regulated interfacial polymerization process to improve acid-resistant nanofiltration membrane permeance, J. Membr. Sci. 641 (2022), 119882.
[20] C. Buten, L. Kortekaas, B.J. Ravoo, Design of active interfaces using responsive molecular components, Adv. Mater. (2019), 1904957.
[21] L. Loske, K. Nakagawa, T. Yoshioka, H. Matsuyama, 2D nanocomposite membranes: water purification and fouling mitigation, Membranes 10 (2020) 295.
[22] X.J. Kong, C. Peng, Y.H. Lan, W. Li, S.S. Chi, C. Zheng, L. Dong, X.H. Wang, Boronate decorated membrane via atom transfer radical polymerization for separation and enrichment of polyphenols from tea drinks, Analytical Methods, 2019.
[23] T. Zhang, W. Huang, T. Jia, Y. Liu, S. Yao, Ionic liquid@β-cyclodextrin-gelatin composite membrane for effective separation of tea polyphenols from green tea, Food Chem. (2020), 127534.
[24] H. Dong, L. Wu, L. Zhang, H. Chen, C. Gao, Clay nanosheets as charged filler materials for high-performance and fouling-resistant thin film nanocomposite membranes, J. Membr. Sci. 494 (2015) 92–103.
[25] B.S. Lalia, V. Kochkodan, R. Hashaikeh, N. Hilal, A review on membrane fabrication: structure, properties and performance relationship, Desalination 326 (2013) 77–95.
[26] G.S. Lai, W.J. Lau, P.S. Goh, A.F. Ismail, N. Yusof, Y.H. Tan, Graphene oxide incorporated thin film nanocomposite nanofiltration membrane for enhanced salt removal performance, Desalination 387 (2016) 14–24.
[27] K.S. Egorova, E.G. Gordeev, V.P. Ananikov, Biological activity of ionic liquids and their application in pharmaceutics and medicine, Chem. Rev. 117 (2017) 7132–7189.
[28] A.S. Amarasekara, Acidic ionic liquids, Chem. Rev. 116 (2016) 6133–6183.
[29] R. Goswami, M. Gogoi, A. Borah, H. Sarmah, P.G. Ingole, S. Hazarika, Functionalized activated carbon and carbon nanotube hybrid membrane with enhanced antifouling activity for removal of cationic dyes from aqueous solution, Environ. Nanotechnol., Monit. Manag. 16 (2021), 100492.
[30] M. Gogoi, R. Goswami, A. Borah, S. Hazarika, In situ assembly of functionalized single-walled carbon nanotube with partially reduced graphene oxide

nanocomposite membrane for chiral separation of β-substituted-α-amino acids, Sep. Purif. Technol. 283 (2022), 120201.
[31] M. Gogoi, R. Goswami, P.G. Ingole, S. Hazarika, Selective permeation of L-tyrosine through functionalized single-walled carbon nanotube thin film nanocomposite membrane, Sep. Purif. Technol. 233 (2020), 116061.
[32] M. Gogoi, R. Goswami, A. Borah, H. Sarmah, P. Rajguru, S. Hazarika, Amide functionalized DWCNT nanocomposite membranes for chiral separation of the racemic DOPA, Sep. Purif. Technol. 279 (2021), 119704.
[33] R. Goswami, M. Gogoi, H.J. Borah, P.G. Ingole, S. Hazarika, Biogenic synthesized Pd-nanoparticle incorporated antifouling polymeric membrane for removal of crystal violet dye, J. Environ. Chem. Eng. 6 (2018) 6139–6146.
[34] K. Baruah, S. Hazarika, Separation of acetic acid from dilute aqueous solution by nanofiltration membrane, J. Appl. Polym. Sci. 131 (2014).